We are IntechOpen, the world's leading publisher of Open Access books Built by scientists, for scientists

4,800
Open access books available

122,000
International authors and editors

135M
Downloads

Our authors are among the

154
Countries delivered to

TOP 1%
most cited scientists

12.2%
Contributors from top 500 universities

CLARIVATE ANALYTICS BOOK CITATION INDEX INDEXED

WEB OF SCIENCE™

Selection of our books indexed in the Book Citation Index in Web of Science™ Core Collection (BKCI)

Interested in publishing with us?
Contact book.department@intechopen.com

Numbers displayed above are based on latest data collected.
For more information visit www.intechopen.com

13

Optical Amplifiers from Rare-Earth Co-Doped Glass Waveguides

G. Vijaya Prakash[1], S. Surendra Babu[2] and A. Amarnath Reddy[1]
[1]*Nanophotonics lab, Department of Physics, Indian Institute of Technology, Delhi, New Delhi-110016,*
[2]*Laser Instrumentation Design Centre, Instruments Research & Development Establishment, Dehradun-248 008, India*

1. Introduction

Optical amplifiers are of potential use in wide variety of optoelectronic and optical communication applications, particularly for Wavelength Division Multiplexing (WDM) to increase the number of channels and transmission capacity in optical network systems. For efficient performance of WDM systems, essential requirements are larger bandwidth, higher output power and flat gain over entire region of operation. Recent research is focused on design and development of fiber/MEMS-compatible optical amplifiers. Some examples of such sources are semiconductor quantum dot light-emitting diodes, super-luminescent diodes, Erbium doped fibre amplifier (EDFA, 1530-1625nm), Erbium doped planar amplifier (EDWAs), Fibre Raman amplifier, Thulium doped fibre amplifier (1460-1510nm). However, for many applications covering the total telecommunication window (1260-1700nm) is highly desirable and as such it is not yet realized. Typical attenuation spectrum for glassy host is shown in Figure 1. Specially the low loss region extending from 1450 to 1600 nm, deemed the 3rd telecommunication window, emerged as the most practical for long haul telecommunication systems. This window has been split into several distinct bands: Short-band (S-band), Centre-band (C-band) and Long-band (L-band). With several generations of development, the transmission rates have increased dramatically so that several Terabits per second data can be transmitted over a single optical fiber at carrier wavelengths near 1550 nm, a principal optical communication window in which propagation losses are minimum. EDFAs are attractive to WDM technology to compensate the losses introduced by WDM systems and hence has grown as a key to upgrade the transmission capacity of the present fiber links. EDFAs are widely used in long-haul fiber optic networks where the fiber losses are limited to 0.2 dB/km, is compensated periodically by placing EDFAs in the transmission link with spacing of up to 100 km. EDFAs make use of trivalent erbium (Er^{3+}) ions to provide the optical amplification at wavelengths near 1550 nm, the long wavelength window dominantly used in optic networks since the fiber losses are found minimum around this wavelength. Light from an external energy source at a wavelength of 980 nm or 1450 nm, coupled along with the information signal, and is passed through the EDFA to excite the Er^{3+} ions in order to produce the optical amplification through stimulated emission of photons at the signal wavelength. Er^{3+} doped waveguides (EDWA) have

obvious advantages as short-length devices and can be integrated monolithically or in hybrid form. Thus individual or co-doped rare earth doped glass fibres/waveguide research is of great promise and concentrated mostly on silicate glasses. However, their Amplified Spontaneous Emission (ASE) bandwidth is limited and also intrinsic absorption occurs even in its most pure form and is associated with the vibrational characteristics of the chemical bonds such as silicon-oxygen bonds. Recently, rare earth co-doped fluoride and tellurite glasses have shown considerable ASE with extended bandwidth, where the emission broadness arises due to inter-ion energy transfer. Overall, the specific technological information related to suitability of rare earth doping, and proper choice of glass matrix is still not clear and worthy of pursuit.

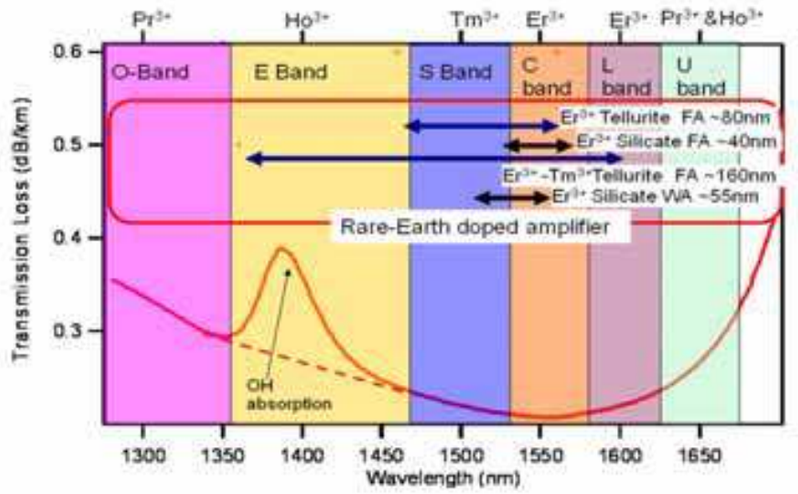

Fig. 1. Loss characteristics of silica fiber and emission bands of some rare earth ions in different glass hosts.

In general, application and utilities of glassy materials are enormous and are governed by the factors like composition, refractive index, dopants/impurities present in the glasses. Demanding physical features of rare earth doped fibers/waveguide devices are (1) high solubility of rare earth for large concentration doping, (2) large temperature gap between the glass transition to crystallization temperature, (3) physical durability such as mechanical and moisture robustness. Moreover, the rare earth emission in glassy matrix is strongly dependent on crystal field effects, local environment where the ion is situated, phonon energies, refractive index and precise details about glass defects (Urbach tails) extended into the band gap. Though silicate glass is inexpensive and most useful matrix for many applications, the low refractive index and strong OH band contributions are major disadvantages. Numerous investigations were made in search for improvised and suitable glass matrix for strong rare earth emission. Among them, phosphate glasses are found to be most suitable for rare earth emission and phosphate glass lasers are already available in the market. However, the knowledge is still largely incomplete due to unusual structural characteristics such as high co-ordinations of the elements present and the large number of chemical elements that are being used in the compositions of these glasses. Our extensive studies on phosphate glasses show wide range of transparency, moisture insensitivity and ability in accepting large amount of rare earths as dopants, and most importantly the compatibility for fibre and waveguides (Vijaya Prakash et al., 2002; Surendra babu et al.,

2007, Pradeesh et al., 2008; Amarnath Reddy et al., 2010). In this chapter we review the essential rare earth spectroscopic details such as absorption analysis through Judd-Ofelt computations, emission lifetimes, gain cross-sections etc,. We further discuss the characteristic features of suitable glass hosts. Finally, we present most common waveguide fabrication techniques and a comparative review of information related to available waveguide devices.

2. Spectral properties of rare earths ions

Optically active rare earth (RE) ions are characterized by their 4f electrons in seven 4f-orbitals. In addition to the most stable electronic configurations (ground state), various configurations with excited higher energy are possible in the thirteen RE ions from Ce^{3+} to Yb^{3+} ion. The energy of these different electronic configurations is separated by the Coulombic spin-orbit and ligand field interactions, resulting in the well-known energy level structures. The energy levels and various absorption and emission transitions of most sought-after Erbium (Er^{3+}) ions are shown in Figure 2A.

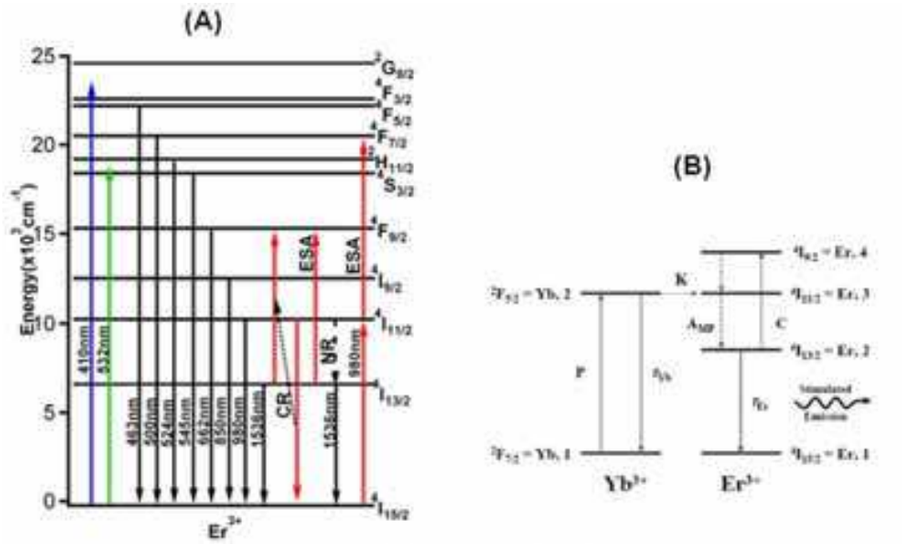

Fig. 2. (A) Partial electronic energy levels and various absorption and emission transitions of Er^{3+} ions and (B) energy transfer between Er^{3+} and Yb^{3+} ions.

The $4f^N$ electron configuration of a rare earth ion is composed of a number of electronic states. The spread of $4f^N$ energy levels arises from various atomic interactions between electrons and can be found by solving the time dependent Schrodinger equation. The weak interaction of the 4*f* electrons with electrons from other ions (in any environment) allows a Hamiltonian to be written for an individual rare earth ion as (Wybourne, 1965).

$$\hat{H} = \hat{H}_{FI} + \hat{H}_{CF} \tag{1}$$

where $\hat{H}_{FI}$ is defined to incorporate the isotropic parts of $\hat{H}$ (including the spherically symmetric part of the 4*f* -electron-crystal-field interactions) and $\hat{H}_{CF}$ is defined to represent the non-spherically symmetric components of the even parity crystal-field. The majority of RE optical absorption transitions occur between states which belong to the $4f^N$ configuration.

For intra-*f* shell transitions the initial and final states have the same parity; this would imply that the electric-dipole process is forbidden (Görler-Walrand et. al., 1998). However, in cases where the site symmetry is not a centre of inversion (as usually the case of the glass), the site interaction Hamiltonian can contain odd-parity terms, thereby introducing a degree of electric-dipole strength into the intra-*f* –shell transitions. Using some simplifications, Judd and Ofelt have provided a way to treat conveniently the spectral intensities of intra-configurational transitions of 4*f* ions in solids (Judd, 1962; Ofelt, 1962).
The experimental oscillator strengths of the absorption spectral transitions are calculated from (Reisfeld et al., 1977)

$$f_{\exp} = \frac{2303mc^2}{N\pi e^2}\int \varepsilon(\bar{\nu})d\bar{\nu} \tag{2}$$

where m and e are the electron mass and charge respectively, c is the velocity of light and $\varepsilon(\bar{\nu})$, the extinction coefficient and is given by $\varepsilon(\bar{\nu}) = \left(1/cl\right)\log\left(I_0/I\right)$ where c is concentration of RE ion in moles/litre, l is the optical path length (cm) and $\log(I_0/I)$ is the absorptivity. According to Judd-Ofelt (JO) theory the oscillator strengths for an induced electric dipole transition can be calculated theoretically from the relation

$$f_{cal} = \sigma\sum T_\lambda \left\langle f^N\psi J\middle|U^\lambda\middle|f^N\psi' J\right\rangle^2 \tag{3}$$

Where $T_\lambda = \tau_\lambda(2J+1)^{-1}$, σ is the mean energy of the transition in cm^{-1}, T_λ are the adjustable Judd-Ofelt parameters and the U^λ are doubly reduced unit matrix elements. Since these matrix elements are insensitive to ion environment, free ion matrix elements are used from literature. The experimental oscillator strengths were least square fit to obtain the intensity parameters T_λ. These parameters are used in turn to calculate Ω_λ (λ = 2, 4 and 6) using the expression,

$$\Omega_\lambda(cm^2) = \frac{3h}{8\pi^2 mc}\frac{9\eta(2J+1)T_\lambda}{(\eta^2+2)^2} \tag{4}$$

where η is the refractive index of the medium, (2J+1) is the degeneracy of the ground level of the particular ion of interest.
In general, the oscillator strengths and positions of given transitions are sensitive to the local environment of RE ion sites occupied within the glass network. Therefore, JO parameters provide critical information about the nature of bond between RE ions to the surrounding ligands, particularly Ω_2 parameter is sensitive to the local environment of RE ions and is often related to the asymmetry of the coordination structure, the polarizability of ligand ions and nature of bonding. On the other hand the values of Ω_4, and Ω_6 values, depend on bulk properties such as viscosity and dielectric of the media and are also effected by the vibronic transitions of the rare earth ions bound to the ligand atoms (Vijay Prakash et al., 2000).
Accurate knowledge of absorption and emission cross sections is required for a range of applications, such as modelling of optical amplifiers and fiber lasers. While it is not straightforward to measure both of these cross sections accurately, owing to complications such as spectral re-absorption, up-conversion, excited-state absorption etc. The theory of

McCumber (McCumber, 1964) is a powerful tool that permits one of these two cross sections to be calculated if the other is known from measurements. The radiative transition probability between the states ψ J and ψ 'J' is given by

$$A(\psi J,\psi' J') = \frac{64\pi^4 \overline{\upsilon^3}}{3h(2J+1)}\left[\frac{\eta\left(\eta^2+2\right)^2}{9}S_{ed} + \eta^3 S_{md}\right] \tag{5}$$

where S_{ed} and S_{md}, are the electric and magnetic dipole line strengths respectively given by

$$S_{ed} = e^2 \sum_{2,4,6} \Omega_\lambda \left\langle \psi J \middle\| U^\lambda \middle\| \psi' J' \right\rangle^2 \tag{6}$$

and

$$S_{md} = \frac{e^2 h^2}{16 m^2 c^2 \pi^2}\left\langle \psi J \middle\| L + 2S \middle\| \psi' J' \right\rangle^2 \tag{7}$$

The total radiative probability $A_T(\psi J)$, the radiative life time (τ_R), branching ratios(β_R) and stimulated emission cross sections(σ_p) are given by

$$A_T(\psi J) = \sum A(\psi J,\psi' J') \tag{8}$$

$$\beta_R = A(\psi J,\psi' J') / A_T(\psi J) \tag{9}$$

$$\tau_R = (A_T(\psi J))^{-1} \tag{10}$$

and

$$\sigma_p(\lambda_p) = \frac{\lambda_p^4}{8\pi c \eta^2 \Delta\lambda_p} A\left(\psi j,\psi' j'\right) \tag{11}$$

where λ_p and $\Delta\lambda_p$ are average emission wavelength and effective emission band width respectively.

While Er-doped glasses are of significant interest for C-band telecommunication window, in compact systems active material is often co-doped with Ytterbium (Yb^{3+}) to enhance absorption efficiency. To obtain sufficient population inversion, even at low concentration of Er, large amount of Yb^{3+} sensitizing ions is required. Yb → Er migration-assisted non-radiative energy transfer scheme is shown in Figure 2B. For efficient population of the upper $^4I_{13/2}$ laser level of Er^{3+} ions via Yb^{3+} ions, two indispensable conditions have to be fulfilled. The first one is a rapid excitation relaxation from $^4I_{11/2} \rightarrow {}^4I_{13/2}$ of Er^{3+} ion level is necessary. Otherwise reverse energy transfer back to Yb^{3+} ions in combination with the up-conversion processes will compete the upper laser level population process. This may lead to reduction in efficiency, or even inhibit of 1550nm emission completely. Second one is the quantum yield of the upper laser level $^4I_{11/2}$ luminescence should be high. Both conditions are well satisfied in phosphate glasses where Er^{3+} ion luminescent lifetimes are typically τ_1=7.8 - 9.0ms for the $^4I_{13/2}$ level and $\tau_2 \cong$ 1–3 μs for the $^4I_{11/2}$ level (Zhang et al., 2006; Liang et al., 2005)

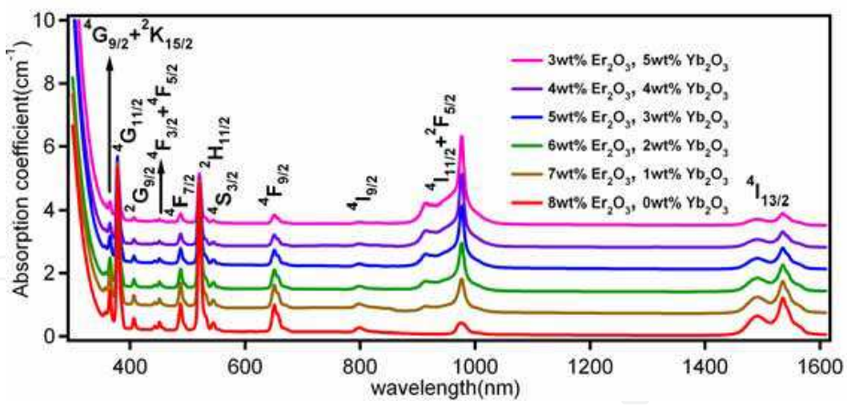

Fig. 3. Typical absorption spectra of Er^{3+}/Yb^{3+} co-doped phosphate (NAP) glasses.

The absorption spectra of Er^{3+}/Yb^{3+} co-doped NAP ($Na_3Al_2P_3O_{12}$) phosphate glass are shown in Figure 3 (Amarnath Reddy et al, 2010). The spectra consist of absorption bands corresponding to the transitions from the ground state $^4I_{15/2}$ of Er^{3+}ions. From the absorption spectral analysis three important JO parameters (Ω_λ = 2, 4 and 6), were obtained. As mentioned before, both covalence and site selectivity of RE ion with non-centro symmetric potential contributes significantly to Ω_2. The variation of Ω_2 with Er^{3+} concentration in various phosphate glasses is shown in Figure 4A and also in Table 1. Also, Ω_2 is strongly dependent on the hypersensitive transitions. Hypersensitivity is related to the covalency through nephelauxetic effect and affects the polarizability of the ligands around the rare earth ions (Kumar et al., 2007). Higher ligand polarizability results in a larger overlap between rare earth ions and ligands orbital, i.e., higher degree of covalency between rare earth ions and the ligands. Hypersensitive nature of $^4I_{15/2} \rightarrow {}^2H_{11/2}$, and $^4G_{11/2}$ transitions of Er^{3+} ions, which is strongly dependent on covalency and site asymmetry, governs the radiative properties of Er^{3+} ions. Though Ω_2 parameter can be an indicator for covalent bonding, in view of hypersensitivity, it is appropriate to look at the variation of the sum of the JO parameters with the oscillator strengths of hypersensitive transitions instead of taking a single parameter. Figure 4B compares the plots of $\Sigma\Omega_\lambda$ (λ= 2, 4 and 6), against oscillator strengths of the hypersensitive transitions of Er^{3+} ions doped in various glass systems. Lower oscillator strengths are observed for ionic systems such as fluorides while highly covalent systems such as phosphate, and borate glasses show higher oscillator strengths.

Electronic polarization of materials is widely regarded as one of the most influencing parameter and many physical, linear and nonlinear optical properties of materials are strongly dependent on it. Duffy, Dimitrov and Sakka correlated many independent linear optical entities to the oxide ion polarizability of single component oxides (Dimitrov & Sakka, 1996; Duffy, 1986). This polarizability approach, predominantly gives the insight into the strong relation between covalent/ ionic nature of materials and other optical parameters, such as optical band gap (E_{opt}) (Vijay Prakash 2000). Recently we have related optical band gaps of various binary, ternary and quaternary oxide glasses to the polarizability (of cation) in terms of 1-R_m/V_m,(R_m=molar refractivity and V_m= molar volume) known as covalancy parameter or metallization parameter (Pradeesh etal., 2008). Generally, the covalancy parameter ranges from 0.3 to 0.45 for highly polarisable cation containing oxides (such as Pb^{2+} and Nb^{5+}), while for the alkaline and alkaline-earth (such as Na^+, Li^+) oxides it falls in between 0.5-0.70. Although it is quite complex to correlate optical parameters of the glassy

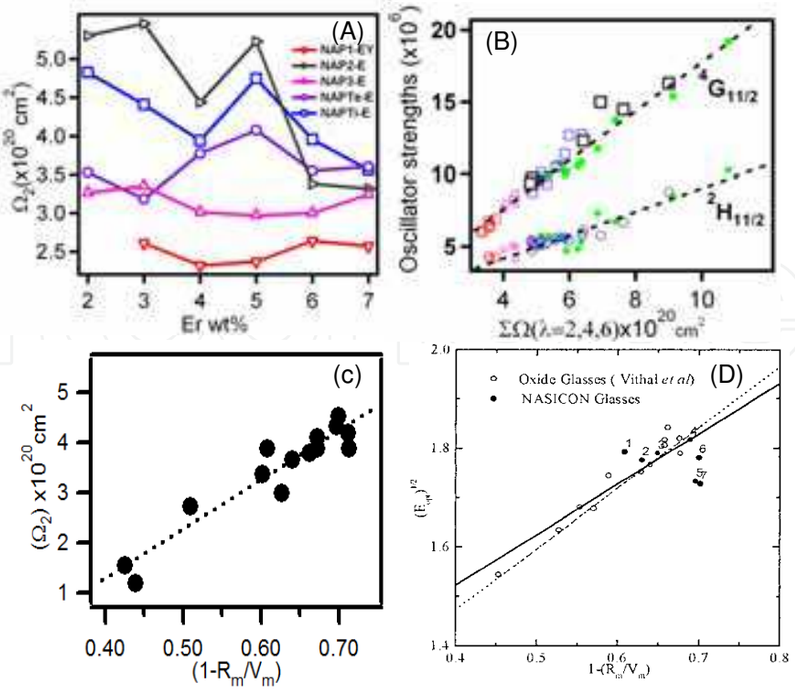

Fig. 4. (A) variation of Ω_2 with Er^{3+} concentration in various phosphate glasses. (B) Oscillator strengths (as open symbols) of various hypersensitive ($^4G_{11/2}$ and $^2H_{11/2}$) and non-hypersensitive ($^4F_{9/2}$ and $^4S_{3/2}$) transitions of Er^{3+} ions with respect to the sum of Judd–Ofelt parameters. Various other glasses are also incorporated (as filled symbols) for comparison (Vijaya Prakash et al., 1999,2000). (C) Ω_2 and (D) E_{opt} values against metallization parameter ($1-R_m/V_m$) (Pradeesh etal 2008,Vijaya Prakash et al., 1999,2000).

Phosphate glass composition	Ω_2	Ω_4	Ω_6
$92(Na_3Al_2P_3O_{12})$ -(8-x) Al_2O_3-(x)Er_2O_3 x=2	3.26	0.57	0.55
$92(Na_3Al_2P_3O_{12})$ -(8-x) Al_2O_3-(x)Er_2O_3 x=3	3.25	0.54	0.55
$92(Na_3Al_2P_3O_{12})$ -(8-x) Al_2O_3-(x)Er_2O_3 x=4	3.01	0.51	0.56
$92(Na_3Al_2P_3O_{12})$ -(8-x) Al_2O_3-(x)Er_2O_3 x=5	2.97	0.49	0.54
$92(Na_3Al_2P_3O_{12})$ -(8-x) Al_2O_3-(x)Er_2O_3 x=6	2.99	0.84	0.59
$92(Na_3Al_2P_3O_{12})$ -(8-x) Al_2O_3-(x)Er_2O_3 x=7	3.24	0.80	0.71
$92(Na_3Al_2P_3O_{12})$ -(8-x) Al_2O_3-(x)Er_2O_3 x=8	3.53	0.76	0.56
$92(Na_2AlP_5O_{15})$ -(8-x) Al_2O_3-(x)Er_2O_3 x=7	3.08	0.80	0.39
$92(Na_2AlP_5O_{15})$ -(8-x) Al_2O_3-(x)Er_2O_3 x=8	3.39	0.72	0.50
60 $PbCl_2$ - 40P_2O_5, 1wt% Er^{3+}	3.36	0.51	1.51
10Na_2O- 50 $PbCl_2$ - 40P_2O_5, 1wt% Er^{3+}	4.11	0.47	1.16
20Na_2O- 40 $PbCl_2$ - 40P_2O_5, 1wt% Er^{3+}	3.66	0.34	1.86
30Na_2O- 30 $PbCl_2$ - 40P_2O_5, 1wt% Er^{3+}	3.79	0.13	1.21
$Na_3TiZnP_3O_{12}$ 1wt% Er^{3+}	4.94	1.15	5.77
$Na_4AlZnP_3O_{12}$ 1wt% Er^{3+}	3.77	1.34	1.25

Table 1. Judd Ofelt ((Ω_λ = 2, 4 and 6) x 10^{-20}, cm^2) parameters for various phosphate glasses

systems with polarizability of oxide ions, it is interesting to see the influence of cation (such as Na^+) polarizability on other independent parameters, such as JO parameters. Since Ω_2 values are known to show dependence on covalent nature of phosphate host, we made a plot between Ω_2 and E_{opt} values against metallization parameter ($1-R_m/V_m$) in Figure 4C&D. Interestingly, the Ω_2 values are monotonically increasing with the metallization parameter. Though with respect to metallization parameters they show more of alkali oxide nature, significantly higher Ω_2 indicates strong covalent nature, could possibly be due to the increased role of phosphate linkage, having more double bonded oxygens (DBOs) coordinated to the rare earth ions.

Further, table 2 gives the most useful physical and spectral parameters, viz., values of density(d, gm/cm^3), Refractive index (n), Judd-Oflet parameters ((Ω_λ, λ=2,4,6)x10^{-20}, cm^2), calculated (τ_{cal}, ms) and measured life times (τ_{exp}, ms), effective line widths ($\Delta\lambda$, nm), absorption (σ_ax10^{-21}, cm^2) and emission cross-sections (σ_ex10^{-21}, cm^2) of Er^{3+} and Er^{3+}/Yb^{3+} doped in phosphate, Tellurite and silicate glasses.

Composition	RE	d/η	Ω_2	Ω_4	Ω_6	τ_{exp}	τ_{cal}	$\Delta\lambda$	σ_a	σ_e	Reference
Phosphate											
$20Na_2O–2Al_2O_3–xEr_2O_3–yYb_2O_3–30Nb_2O_5-15TiO_2–30P_2O_5$	Er^{3+}-Yb^{3+}	-/1.84	-	-	-	3.00	-	53	-	-	Bozelli et al., 2010
Schott	Er^{3+}-Yb^{3+}	-/1.52	-	-	-	9.18	9.21	40	-	-	Zhang, et al., 2006
EYDPG	Er^{3+}-Yb^{3+}	-	-	-	-	7.91	9.10	42	6.56	7.20	Liang, et al., 2005
$72P_2O_5-8Al_2O_3-20Na_2O$	Er^{3+}	-/1.51	6.84	1.94	1.29	-	7.46	-	7.41	8.23	Gangfeng, et al., 2005
WM-1	Er^{3+}-Yb^{3+}	2.83/1.53	6.45	1.56	0.89	7.90	9.10	42	6.56	7.20	Bao - Yu, et al., 2003
$67P_2O_5-14Al_2O_3-14Li_2O-1K_2O$	Er^{3+}-Yb^{3+}	-	7.06	1.70	1.04	8.00	8.62	40	6.4	7.8	Wong, et al., 2002
$29.9Na_2O-30.8P_2O_5-18.7Nb_2O_5-13.9Ga_2O_3-6.6Er_2O_3$	Er^{3+}	-/1.71	3.89	1.00	0.55	8.9	3.10	50	-	-	Righini, et al., 2001
IOG-1	Er^{3+}-Yb^{3+}	-/1.52	6.13	1.48	1.12	8.10	8.55	46	4.13	4.62	Veasey, et al., 2000
Tellurite											
$80TeO_2-10ZnO-10Na_2O-20P_2O_5-0.5Er_2O_3$	Er^{3+}	4.36/1.95	-	-	-	3.90	-	46	6.99	8.50	Fernandez, et al., 2008
$67TeO_2-30P_2O_5-1Al_2O_3-1.75La_2O_3-0.25Er_2O_3$	Er^{3+}	3.75/2.00	3.4	1.0	0.2	4.10	7.90	41	-	6.00	Nandi, et al., 2006
$60TeO_2–30WO_3–10Na_2O$	Er^{3+}	-	7.13	1.90	0.82	3.40	3.46	52	8.10	9.10	Zhao, et al., 2006
$25WO_3-15Na_2O-60TeO_2+(0.05-2Er_2O_3)$	Er^{3+}	-/2.047	6.7	1.7	1.15	2.80	3.39	62	-	-	Conti, et al., 2004
$8Na_2O-27.6Nb_2O_5-64.4Te_2O_5-1Er_2O_3$	Er^{3+}	4.98/2.12	6.86	1.53	1.12	3.02	2.90	-	8.63	1.02	Lin, et al., 2003
Silicate											
$52.0SiO_2·33.0B_2O_3·7.7Na_2O·4.0CaO·2.7Al_2O_3.0.6CeO_2$	Er^{3+}	1.98/1.46	8.15	1.43	1.22	6.00	9.10	45	-	5.10	Ning, et al., 2006
$61.4SiO_2–11.73Na_2O–9.23CaO–16.67Al_2O_3–0.33P_2O_5-0.51K_2O-0.39Er_2O_3$	Er^{3+}	2.624/ 1.54	7.15	1.95	1.01	6.20	8.43	48	-	7.70	Berneschi, et al., 2005
$61SiO_2–12Na_2O–3Al_2O_3–12LaF_3–12PbF_2$	Er^{3+}	3.62/1.66	-	-	-	10.5	-	48	7.50	7.80	Shen, et al.,2004
$73SiO_2–14Na_2O–11CaO–1Al_2O_3–0.4P_2O_5–0.6K_2O$	Er^{3+}-Yb^{3+},	-/1.53	4.89	0.77	0.50	-	-	-	-	-	Righini, et al., 2001
IOG-10	Er^{3+}-Yb^{3+}	-/1.54	-	-	-	10.2	17.8	32	5.70	5.80	Peters, et al., 1999

Table 2. Important spectroscopic parameters of Er^{3+} and Er^{3+}/Yb^{3+} doped various phosphate, tellurite and silicate glasses.

3. Glasses for rare earth based amplifiers

Improvements in the quantum efficiency of the luminescent levels of RE ions can be achieved by selecting a suitable host material and by modifying the local environment surrounding them (Görler-Walrand et. al., 1998). Such modifications are often achieved by breaking up the structure of atoms surrounding a rare earth ion with other, often larger elements, termed as *network modifiers*. Discussing the role of network modifiers requires an understanding of the basic structure of different glass network formers. Oxide glasses, such as borate, silicate, tellurite and phosphate glasses, have proven to be the appropriate host materials for the development of optoelectronic components. Among the oxide glass hosts, phasephate glasses have attracted much attention due to their high transparency, thermal stability, good RE ion solubility, easy preparation in large scale, shaping and cost effective properties. Let us compare the structural features of phosphate glass with well-known silica and tellurite glass networks.

3.1 Silicate glass

Silica is built from basic structural units, the most common of which is the network former unit, $(SiO_4)^{2-}$. This network former consists of a silicon atom at the centre of a tetrahedron with an O atom bonded to each corner. The basic structure of silica glass, Figure 5A, contains tetrahedral units that are tightly connected by their corners through oxygen atoms (bridging oxygens); these random connections form a 3 dimensional structure similar to that shown in the Figure 5B. The strong electron bond which exists between the silicon and oxygen atoms gives the silica glass its impressive mechanical strength and thermal properties. However, the drawback to the silica glass network is its limited soluability of rare earth ions (<3wt%). One explanation of this phenomenon is that rare earth ions require co-ordination of a sufficiently high number of non-bridging oxygens to screen the electric charge of the ion, whereas highly rigid silica glass network cannot co-ordinate the non-bridging oxygens resulting in a system with a higher enthalpy state. Therefore, rare earth ions tend to share non-bridging oxygens to reduce the excess enthalpy, resulting in the

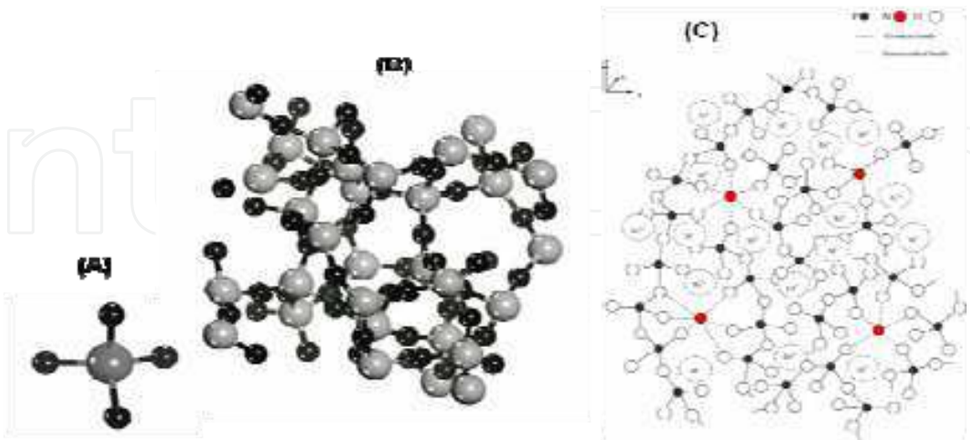

Fig. 5. (A) &(B)Tetrahedral structure of $(SiO_4)^{2-}$, showing 4 oxygen atoms surrounding the central silicon atom and 3 - dimensional structure of SiO_2 , showing the interconnection of the tetrahedral units. (C) Schematic view of the phosphate glass network showing the different type of atoms neighbourhoods.

formation of clusters. To accommodate greater amounts of rare earth ions, network modifiers are required to increase the number of available non-bridging oxygen ions in the silica glass network. Network modifiers such as Na^{3+} and Al^{3+} are often used to facilitate the incorporation of rare earth ions, as their size is substantially greater than the basic network. These modifiers act to break the bridging oxygens to form non-bridging oxygens which can be used to co-ordinate the rare earth ions. Of the network modifiers studied in silica glass to date, Al_2O_3 has shown the most favourable characteristics. Al_2O_3 has also been used to improve the efficiency of Er^{3+} -doped fibre amplifiers by eliminating the quenching effects from the $^4I_{13/2} \rightarrow {}^4I_{15/2}$ transition (Corradi et al., 2006).

3.2 Tellurite glass

Recent work on the structure of tellurite glasses has concluded that the network more closely resembles paratellurite (α-TeO_2), where [TeO_4] units are only linked at their corners (Stavrou et al., 2010). Combining TeO_2 with network modifiers (such as Na_2O) and intermediates (such as ZnO) results in structural modification to chain like structures. In general the tellurite glasses follow the pattern of crystalline α-TeO_2, which are formed by [TeO_4] groups as trigonal bipyramids. Such structural units can progressively form [TeO_{3+1}] and trigonal pyramids [TeO_3] (Surendra babu et al., 2007). Upon network modified, the glass network becomes more open and more non-bridging oxygens are created (Golubeva, 2003; Vijaya Prakash et al., 2001). Tellurite glasses are very promising materials for up-conversion lasers and nonlinear applications (such as photonic crystal fibers) in optics due to some of their important characteristic features such as high refractive index, low phonon maxima and low melting temperatures. Recently, an addition of oxides of heavy metals such as Nb, Pb and W to tellurite glasses is being studied extensively because such additions seem to show remarkable changes in both physical and optical properties of these glasses (Vijaya Prakash et al, 2001).

3.3 Phosphate glass

The structure of phosphate glass consists of random network of phosphorous tetrahedra. In glassy and crystalline phosphate the basic building blocks are PO_4 tetrahedra. In a pure phosphate glass the tetrahedra are linked through three of the oxygens while the fourth oxygen is doubly bonded to the phosphorus atom and does not participate in the network formation. The networks of phosphate glasses can be classified by the oxygen to phosphorus ratio, which sets the number of tetrahedral linkages (through bridging oxygens) between neighboring P-tetrahedra (Vijaya Prakash & Jaganaathan, 1999). When the modifier cations are added to the phosphate glasses, the P=O of phosphate group is unaffected and depolymerization takes place through the breaking linkages only. When a glass modifier (oxides, such as Al_2O_3) is added the network breaks up creating non bridging oxygens in the structure which coordinate the metal ions of the modifier oxide, Figure 5C. With increasing amount of modifier, the number of non-bridging oxygens, per PO_4 unit, will go from zero to three for orthophosphates. At this composition the host structure consists principally of chains of corner linked PO_4 tetrahedra with 2 non-bridging oxygens per tetrahedron. The metal ions of the modifier oxide will not participate in the network but will associate to the non-bridging oxygens (Seneschal et al., 2005).

In recent days NASICON type phosphate glasses (acronym for the crystalline Na-Super-Ionic Conductor, $Na_{1+x}Zr_2P_{3-x}Si_xO_{12}$) has attracted much attention, as they facilitate a large scope for preparing a number of glasses with variation in their constituent metal ions and

compositions. These glasses have the general formula $A_mB_nP_3O_{12}$ where A is an alkali or alkaline earth metal ion and B is one or more metal ions in tri, tetra or pentavalent state. Constituent metal ion variation in these glasses has shown marked changes in Physical, linear and nonlinear optical properties (Mariappan et al, 2005, 2005, et al, Vijaya Prakash et al., 1999,00,01,02). It is also interesting to note that the rare earth ions in NASICON glasses are likely to be located in the sites of A and B, implies that the rare earth oxides are actively involved in glass network than as simple dopants. Morever, due to the presence of alkali ions, the rare earth solubility improves leading to the possibility of using a high concentration of dopants, which is very important for short length optical amplifiers,and further provides suitability for the fabrication of optical wave guide devices by ion exchange. Also chloro/fluorophosphate glasses show potential as hosts for lasers and holographic gratings, specially lead-bearing fluorides are considered to be good candidates for up-conversion studies (Pradeesh et al, 2008, Vijaya Prakash, et al 1999).

Phosphate laser glass is an attractive amplifier material because it combines the required properties of good chemical durability, high gain density, wide bandwidth emission spectrum of erbium, and low up-conversion characteristics (Miniscalco, 1991). Phosphate glass exhibits a high gain density due to a high solubility for rare earth ions. The high ion density results in a significantly short-length optical gain device than silica bsed glass counterparts. For example, Erbium doped silica fiber is typical gain coefficients are about of 2 to 3 dB/m, whereas in phosphate glass waveguide it is about 2 to 3 dB/cm. Erbium-ytterbium doped phosphate glass technology, in particular, has demonstrated a significant capacity for large gain per length coefficients in addition to providing the ability to tailor the absorption by the ytterbium concentration. These combined aspects of the phosphate glass material, and reported results, Table2, support it as a prime candidate for producing compact photonic modules employing gain.

4. Erbium doped waveguide fabrication

As discussed earlier, glass is of particular interest for integrated optics because of relatively low cost, excellent transparency, high optical damage threshold and availability in substantially large sizes. It is rigid and amorphous which makes it easier to produce polarization-insensitive components. Refractive index can be tailored close to that of optical fiber to reduce the coupling losses between the waveguides and optical fibers. There are various waveguide fabrication methods available for waveguides amplifiers such as Ion Implantation of Er ions directly into the pre-fabricated waveguide (Bentini et al., 2008), Thin film techniques (RF Sputtering/PECVD/EBVD) combined with photolithography, reactive ion etching (RIE) and flame hydrolysis (Shmulovich, et. al., 1992; Nakazawa & Ktmuraa, 1992). Composite erbium-doped waveguides (Honkanen et. al., 1992,) and sol-gel based low-cost integrated optoelectronic devices are some of the other interesting developments (Najafi et. al., 1996; Milova et. al., 1997).

Micromachining of glass substrates by high-power femtosecond laser pulses is one of the recent developement in the fabrication of optical channel waveguides, Figure 6C. This technique has an unique advantage in fabricating of 3-D waveguides inside glass substrates, which is not easy from conventional ion-exchange and photolithographic processes. Channel waveguides written using ultrafast lasers in erbium-doped phosphate glasses for integrated amplifiers and lasers operating in the C-band have been already demonstrated (Osellame, 2003).

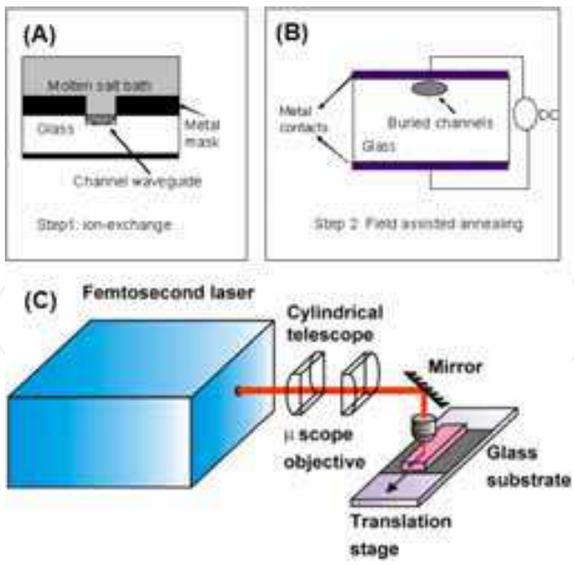

Fig. 6. (A&B) Ion exchange field assisted annealing channel waveguide fabrication (C) Optical setup for femtosecond laser waveguide writing

Among all, ion-exchange has been the most popular technique for rare earth doped waveguides in glass. Molten salt bath has been used as a source of ion-exchange for fabrication of glass waveguides (Ramaswamy & Srivastava, 1988). In this process usually the ion-exchange take place between alkali ions (mostly Na^+) of the glass host and monovalent cations (C_S^+, Rb^+, Li^+, K^+, Ag^+ and Tl^+) from molten salt bath. Alkali containing phosphate glasses are of right choice because of high solubility of rare earth ions without significant reduction in the emission life times. Moreover, many oxide based glasses exhibit poor chemical durability during ion-exchange waveguide fabrication, due to their weak structural network that results into damage of surfaces. Phosphate glasses are considerably stable to thermal and chemical induced fluctuations among other oxides. Ion exchange involves a local change in composition which is brought about by mass transport driven by thermal or electric field gradients or some combination of the two, using lithographically designed mask. Usually, the ion exchange process has no effect on the basic structure of glass network if it is carried out at temperatures well below the softening point of the glass. The ion exchange can be purely a thermal diffusion process, or an electric field assisted diffusion process. The refractive index change and diffusion depth can be controlled easily by proper choice of the exchanged ions and the glass compositions. Table 3 gives ion-exchange conditions for phosphate, tellurite and silicate glass compositions along with refractive index change and diffusion depths. The index profile can be tailored from shallow graded to a step like function with the assistance of electric field. For slightly buried waveguides, field assisted one step or two step ion exchange processes is often used, (Figure 6A&B) (Liu and Pun, 2007). This technique has already well-demonstrated the capacity to form planar and channel waveguides as power splitters, multiplexers, optical amplifiers (EDWAs), with integrated-optical functions with great stability and low losses.

The depth of the waveguide d is related the diffusion time t (time of the ion-exchange process) by the equation $d = \sqrt{D.t}$ where D is the effective diffusion coefficient which depends on the molten salt solution, the glass and the temperature. This kind of diffusion profile indicates that the mobility of the incoming alkali ion (example, Ag^+) is much lower

than that of the original ion (example, Na^+) in the glass. Furthermore, the diffusion coefficient shows an Arrhenius temperature dependence:

$$D = D_0 \exp\left[-\frac{E_D}{RT}\right] \tag{12}$$

where D_0 is a fitting constant, E_D is the activation energy, T is the temperature of the bath and R is the universal gas constant (8.314 J/K mol).

A successful ion-exchange process to fabricate stable and low-loss waveguides demands (1) control of host glass composition and identifying suitable processing conditions, (2) increased ASE cross sections with high gain flatness, (3) high refractive index and low-loss glass hosts with a compatibility for efficient emission, and (4) complete understanding of guest-host interaction in rare earth doped glass.

Composition	Melt composition	RE	T⁰C	Time	η	Δη	d μm	D.C. m²/S	Reference
Phosphate									
$20Na_2O–(5-x-y)Al_2O_3–xEr_2O_3–yYb_2O_3–30Nb_2O_5–15TiO_2–30P_2O_5$	97.33g $NaNO_3$+2.67g $AgNO_3$	Er^{3+}/ Er^{3+}- Yb^{3+}	400	1h	1.836 1.894 1.851	0.007 0.007 0.021	7.50 2.20 7.90	-	Bozelli, et al., 2010
Phosphate IOG-1	5$AgNo_3$+95KNO_3 4.8$AgNo_3$+89KNO_3+6.2$NaNO_3$	Er^{3+}- Yb^{3+}	345 330	35min 8min	-	0.02	7.00	5.8x 10^{-16} 28 x10^{-16}	Jose, et al., 2003
Tellurite									
$25WO_3$-$15Na_2O$-$60TeO_2$+(0.05-$2Er_2O_3$)	2$AgNo_3$+43KNO_3+55$NaNO_3$	Er^{3+}	330	90min	2.03	0.12	-	6x10^{-10}	Conti, et al., 2004
$12Na_2O$ -$35WO_3$ - $53TeO_2$- $1Er_2O_3$	1.0$AgNO_3$ 49.5$NaNO_3$ 49.5KNO_3	Er^{3+}	300 - 360	5h	2.07	0.10	3.30	-	Sakida et al., 2007
$75TeO_2$-$2GeO_2$-$10Na_2O$-$12ZnO$-$1Er_2O_3$	2$AgNo_3$+49KNO_3+49$NaNO_3$	Er^{3+}	250 - 280	3-12h	2.01	0.24	2.21	1.0x10^{-16}	Rivera, et al., 2006
Silicate									
$73SiO_2–14Na_2O–11CaO–1Al_2O_3–0.4P_2O_5–0.6K_2O$ mol%	0.5$AgNo_3$+99.5$NaNO_3$	Er^{3+}- Yb^{3+}	-	-	1.52	0.044	2.1	6x10^{-9} at1.53	Righini, et al., 2001
MM40 $12Na_2O$+ZnO+MgO+ $SiO2+2Er_2O_3$	100KNO_3 for K+↔Na+ 24$AgNO_3$+50$NaNO_3$+50KNO_3 for Ag+↔Na+	Er^{3+}	375 280	2h 5min	-	0.009 0.085	8.20 3.40	3.12x10^{-9} 12.9x10^{-9}	Salavcoca, et al., 2005
$74.3SiO_2–13.4Na_2O–4.4CaO–2.8Al_2O_3–3.2MgO$-$0.5K_2O$-$1.4BaO$	41KNO_3-59$Ca(NO_3)_2$	Pure	380	6h	-	0.008	9.1	-	Kosikova et al., 1999

Table 3. Ion-exchange waveguide characteristic parameters, substrate refractive index (n), change in refractive index (Δn), depth (d,μm) of waveguide and diffusion coefficient (DC,m²/s) of melt composition, temperature (°C) and time used for various phosphate, tellurite and silicate, glass waveguides.

5. Spectroscopic and waveguide characterization

5.1 Prism coupling

Prism coupling technique is widely considered as one of the effective ways to characterise planar optical waveguides. The totally reflecting prism coupler technique, also known as the ***m***-line technique, is commonly used to determine the optical properties of thin films. The coupling of an incident laser beam by a prism into a planar waveguide is governed by the

incident angle θ of the beam on the prism base. Under total internal reflection conditions, coupling of light into the waveguide would occur via resonant frustrated total reflection, i.e. via evanescent waves in the air layer (Figure 7A). Such coupling occurs only when resonant conditions inside the waveguide are met such phase matching condition. This leads to a finite number of discrete incidences of the light beam, for which the light can be strongly coupled into the waveguide and can be transmitted through the substrate. In the experiment, the resonant coupling of the laser beam into the waveguide is observed through the appearance of dark and bright lines in the reflected beam known as ***m***-lines, Figure 7B. Effective index of each guided mode in a waveguide is calculated by

$$n_{eff} = n_p \sin\left(\theta_p + \sin^{-1}\left(\sin\theta_m / n_p\right)\right) \tag{13}$$

here n_p is the prism index, θp is the angle of prism and θ_m is the synchronised angle. From the measured refractive index profile, one can estimate the information of waveguide, such as the depth, the change in refractive index and the number of modes coupled to the waveguide. The most popular method for refractive-index profiling of planar waveguides is the inverse Wentzel–Kramer–Brillouin (WKB) method, in which the refractive-index profile of a waveguide is defined uniquely by the relationship between the effective index and the mode order, i.e., the effective-index function (Chiang, et. al., 2000).

5.2 Spectroscopic properties

The relative absorption and emission cross sections at both pump and signal wavelengths are obtained from the absorption and emission measurements, as mentioned earlier. For intensity profile of the guided modes and scattering losses, light will be fed through butt-coupling fiber coupled to a tunable laser source through the channels of edge- polished waveguides. The mode field profiles at the signal and pump wavelengths are obtained by near-field IR imaging at the waveguide output facets. The channel waveguide scattering loss are estimated from the Fabry–Perot resonator method (Lee, 1998) and propagation losses can be estimated from the conventional cutback method.

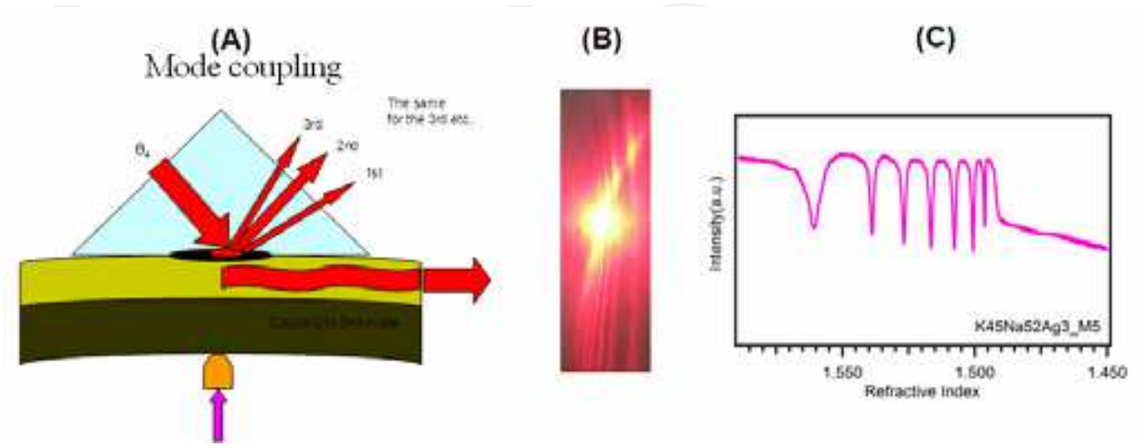

Fig. 7. (A) Schematic representation of prism coupling, (B) photograph of *m*-line pattern and (C) *m*-line intensity spectra as a function of effective refractive index.

The small signal gain or optical gain measurements are usually performed from the typical experimental setup showin in Figure 8, consists of a tunable laser (signal) and a semiconductor laser diode (pump) as shown in Figure 8. The signal and pump lasers are combined by a suitable fiber WDM and coupled into the waveguides using a single mode fiber. At the waveguide output facet, the amplified signal will be conveniently separated from the pump in the second fiber WDM coupler and the eventual signal is detected using a detector or optical spectrum analyzer. The signal light intensities from the output of the waveguide with and without pump laser were measured to estimate the internal gain G_{INT} (= signal light power with pump/signal light power without pump).
The optical gain G_O, relative gain G_R (signal enhancement), and net gain G_N of the waveguide amplifier are defined as

$$G_O = 10\log_{10}\left(P_{\text{Sig (pump ON)}}/P_{\text{sig (pump OFF)}}\right) \tag{14}$$

$$G_R = 10\log_{10}\left((P_{\text{Sig (pump ON)}} - P_{ASE})/P_{\text{sig (pump OFF)}}\right) \tag{15}$$

$$G_N = G_R\text{-coupling losses-waveguide losses-RE}^{3+}\text{ absorption losses} \tag{16}$$

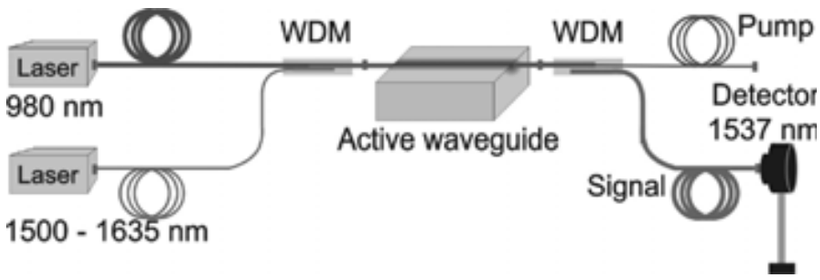

Fig. 8. Experimental setup for Er doped waveguide optical gain measurements

In order to obtain the net gain, it is reasonable to use the following three approaches for a practical waveguide amplifier. The first one is to decrease the waveguide loss by improving the waveguide quality; the second is to increase the coupling efficiency; and the third one is to enhance the pump power, or improve mode confinement in the guide at both pump and signal wavelengths.

6. Conclusion

A brief review of rare earth-doped glass waveguides and their potential application as optical amplifiers is presented. Significance of spectral information, glass composition and rareearth (RE) ion-glass host interaction for engineering waveguide devices, which can potentially useful to design waveguide devices and/or fully integrated photonic structures is discussed. Further, a brief review on fabrication strategies related to waveguides and the influence of the glass composition and other conditions are also presented. Glass-based waveguides thus offer excellent flexibility in fabricating multi-functional optoelectronic

devices using cost-effective technologies, having adequate knowledge of glass and rare earth properties.

Table 4 gives the optical gain parameters of various phosphate, tellurite and silicate glass waveguides fabricated from different fabrication methods, ion-exchange (IE), ion exchange filed assisted annealing (IE FAA) and femtosecond laser writing (FSLW). Optical gain parameters includes the coupling losses (CL, dB/facet), propagation losses (α_p, dB), absorption losses (α_a, dB), insertion losses (IL, dB), internal gain (G_{INT}, dB), relative gain (G_R, dB) and net gain (G_N, dB/cm).

Method of fabrication	Channel aperture , laser specification	Length cm	RE	CL dB/facet	α_p dB/cm	α_a dB	IL dB	G_{INT} dB	G_R dB	G_N dB/cm	Gain range (nm)	Reference
Phosphate												
IE,FAA	6μm	1.24 2.72	Er^{3+}-Yb^{3+}	2.20 2.20	2.27 2.22	5.70 28.00	-	- -	7.0	-	1520-1580	Zhang et al., 2006
IE	4-12 μm	3.80	Er^{3+}-Yb^{3+}	-	0.33	-	3.60	-	-	3.65	-	Liang et al.,2005
IE	4-10μm	1.50	Er^{3+}-Yb^{3+}	-	0.80	-	-	-	-	3.30	-	Wong et al., 2002
IE, FAA	6 μm	4.00	Er^{3+}-Yb^{3+}	0.25	0.30	-	12.2	-	-	2.00	1530-1560	Liu. et al, 2007
IE, FAA	6,8 μm	1.20	Er^{3+}-Yb^{3+}	0.32	0.30	5.40	-	-	-	3.40	-	Liu, et al., 2004
FSLW	150fs,500μJ, 1kHz, 270nJ, 885kHz	2.5 2.2	Er^{3+}-Yb^{3+}	2.4 0.1	0.28 0.4	-	5.5 1.2	1.4 7	-	- 2.72	- 1530-1565	Osellame et al., 2008
FSLW	22MHz,350fs, 1μJ	3.70	Er^{3+}-Yb^{3+}	0.25	0.40	-	1.90	-	-	1.97	1530-1580	Valle, et al., 2005
FSLW	166kHz,300fs, 270nJ	2.00	Er^{3+}-Yb^{3+}	0.25	0.80	-	2.10	4.4	-	1.15	1530-1550	Taccheo, et al., 2004
Tellurite												
FSLW	600kHz,350fs, 1.3μJ	2.50	Er^{3+}	0.50	1.35	2.08	4.40	1.25	-	-	1530-1610	Fernandez, et al., 2008
IE	3μm thick	5.00	Er^{3+}	-	8.00	-	-	-	-	-	-	Sakida, et al., 2006
Silicate												
IE	7-13μm	3.50	Er^{3+}-Yb^{3+}	-	8.00		-	2.50	-	-	-	Righini, et al., 2001
IE	3μm	3.00	-	0.76	0.50	-	2.99	-	-	-	-	He, et al., 2008
IE	3μm	1.80	Er^{3+}-Yb^{3+}	0.36	0.25	-	-	-	-	-	-	Peters, et al., 1999
FSLW	1kHz,100fs, 1-90μJ	1.00	Er^{3+}	0.70	0.90	5.5		2.30	-	-	-	Vishnubhatla, et al., 2009
FSLW	600kHz,350fs, 40-150nJ	1.00	Er^{3+}-Yb^{3+}	0.40	0.34	4.34	5.56	1.93	6.1	0.72	1535-1555	Psaila, et al., 2007
FSLW	5kHz,130fs, 0.3μJ	1.00	Er^{3+}	1.20	1.00	6.90	11.2	1.70	8.6	-	-	Thomsom, et al., 2006
FSLW	5kHz,250fs, 0.9μJ	1.90	Er^{3+}	0.80	1.68				2.7		-	Thomson, et al., 2005

Table 4. Various optical gain parameters of Phosphate, tellurite, Silicate glass waveguides

7. Acknowledgments

Authors acknowledge the financial support from Ministry of Information Technology, India through the project on *"Ultra Wideband Optical Sources from rare earth co-doped glass Waveguides-Fabrication and Characterization "*under Photonics switching Multiplexing and Networking (PSMN) programme-Phase II. This work is partially supported by *UK-India Education and Research Initiative* (UKIERI) programme.

8. References

Amarnath Reddy, A.; Sekhar, C.H., Pradeesh, K., Surendra Babu, S. & Vijaya Prakash, G. (2010). *Optical properties of Dy^{3+}-doped Sodium-Aluminium-Phosphate glasses*. Journal of Materials Science. (Accepted)I *0022-2461*

Amarnath Reddy, A.; Surendra Babu, S. Pradeesh, K., Otton, C. J., &Vijaya Prakash, G. (2010). Optical properties of highly Er^{3+} oped Sodium-Aluminium- Phosphate Glasses for broadband 1.5 μm emission. *(un published)*

Bao-Yu, C.; Shi-Long, Z. & Li-Li, H. (2003). Novel Chemically Stable Er^{3+}-Yb^{3+} Codopded Phosphate Glass for Ion-Exchanged Active Waveguide Devices. *chinese Physics Letter* 20, 11, (July, 2003) 2056–2057, 0256-307x

Bentini, G. B.; Chiarini, M., Bianconi, M., Bergamini, F., Castaldini, D., Montanari, G. B., Bogoni, A., Potì, L., Sugliani, S., Nubil, A., De Nicola, P., Gallerani, L., Pennestrì, G. & Petrini, G. (2008). Waveguide formation by ion implantation in Er doped optical materials. *Nuclear Instruments and Methods in Physics Research B*, 266, (2008) 3120–3124, 0168-538x

Berneschi, S.; Bettinelli, M., Brenci, M., DallIgna, R., Conti, N. G., Pelli, S., Profilo, B., Sebastiani, S., Speghini, A. & Righini, G. C. (2006). Optical and spectroscopic properties of soda-lime alumino silicate glasses doped with Er^{3+} and/or Yb^{3+}. *Optical Materials*, 28, (August, 2006) 1271–1275, 0925-3467

Berneschi, S.; Bettinelli, M., Brenci, M., Conti, G., Pelli, S., Sebastiani, S., Siligardi, C., Speghini, A. & Righini, G.C. (2005). Aluminum co-doping of soda-lime silicate glasses:Effect on optical and spectroscopic properties. *Journal of Non-Crystalline Solids*, 351, (July, 2005) 1747–1753, 0022-3093.

Bozelli, J. C.; De Oliveira Nunes, L.A., Sigoli,F.A. & Mazali, I. O. (2010). Erbium and Ytterbium Codoped Titanoniobophosphate Glasses for Ion-Exchange-Based Planar Waveguides. *Journa of American Ceramic Society*, (2010) 1–4, 0002-7820

Chiang, K. S.; Wong, C. L., Cheng, S. Y. & Chan, H. P. (2000). Refractive-Index Profiling of Graded-Index Planar Waveguides from Effective Indexes Measured with Different External Refractive Indexes . *journal of Lightwave Technology*, 18, 10, (October 2000) 1412-1417, 0733-8724

Conti, G. N.; Berneschi, S., Bettinelli, M., Brenci, M., Chen, B., Pelli, S., Speghini, S., Righini,G.C. (2004). Rare earth doped tungsten tellurite glasses and waveguides: fabrication and characterization. *Journal of Non-Crystalline Solids*, 345&346, (October, 2004) 343–348, 0022-3093

Corradi,A. B.; Cannillo, V., Montorsi, M., & Siligardi, C. (2006). Influence of Al_2O_3 addition on thermal and structural properties of erbium doped glasses. *Journal of Materials Science*, 41, 10, (April, 2006) 2811–2819, 0022-2461

Dimitrov, V. & Sakka, S. (1996). Electronic oxide polarizability and optical basicity of simple oxides. *Journal of Applied Physics*, 79, 3, (February, 1996) 1736-1740, 0021-8979

Duffy, J. A. (1986). Chemical bonding in the oxides of the elements: A new appraisal. *Journal of Solid State Chemistry*, 62, (April,1986) 145-157, 0022-2461, 0022-4596

Fernandez, T. T.; Valle, D. G., Osellame, R., Jose, G., Chiodo, N., Jha, A. & Laporta, P. (2008). Active waveguides written by femtosecond laser irradiation in an erbium-doped

phospho-tellurite glass. *Optics Express*, 16, 19, (September, 2008) 15198-15205, 1094-4087

Gangfeng,Y.; Zhonghong,J., Zaide,D., Bing,Y., Tingzhao,Y. & Zhouming,F. (2005). Effect of Network Modifiers on Spectroscopic Properties of Erbium-doped Phosphate Glasses. *Journal of Wuhan University of Technology - Material Science Education*, 20, 1, (March, 2005) 60-63, 1000-2413.

Golubeva, O.Y. (2003). Structural Interpretation of the Results of Investigations into the Influence of Residual Water on the Properties of One-Alkali Borate Glasses. *Glass Physics and Chemistry*, 29, 6, (June, 2003) 571–574, 1087-6596

Görler-Walrand, C. & K. Binnemans (1998). *Handbook on the Physics and Chemistry of Rare Earths*, Ed. K. A. Gschneidner Jr. and L. Eyring, North-Holland, Amsterdam, 1998, Vol. 25, pp.101

He, Z.; Li, Y., Li, Y., Zhang, Y., Liu, L. & Xu, L. (2008). Low-loss channel waveguides and Y-splitter formed by ion-exchange in silica-on-silicon. *Optics Express*, 16, 5, (March, 2008) 3172-3177, 1094-4087

Honkanen, S.; Najafi, S.I., Wang, W.J. (1992). Composite rare earth-doped glass waveguides. *Electronics Letters*, 28, 8,(April, 1992) 746-747, 0013-5194

Jose, G.; Sorbello, G., Taccheo, S., Cianci, E., Foglietti, V. & Laporta, P. (2003). Active waveguide devices by Ag–Na ion exchange on erbium–ytterbium doped phosphate glasses. *Journal of Non-Crystalline Solids*, 322, (July, 2003) 256–261, 0022-3093

Judd, B. R. (1962). Optical absorption intensity of rare earth ions. *Physical Review*, 127,3, (March, 1962) 750-761, 0031-899x

Kosıkova, J. & Schrofel, J. (1999). Planar waveguides prepared by K^+–Na^+ field-assisted ion exchange in different types of silicate glass. *Journal of Materials research*, 14, 7, (July, 1999) 3122-3129, 0884-2914

Kumar, G.A.; Riman, R. A., Diaz Torres, L. A., Banerjee, S., Romanelli, M. D., Emge, T. J. & Brennan, J. G. (2007). Near-Infrared Optical Characteristics of Chalcogenide-Bound Nd^{3+} Molecules and Clusters. *Chemistry of Materials*, 19, (May, 2007) 2937-2946, 0897-4756

Lee. C.T. (1998). Nondestructive measurement of separated propagation loss for multimode waveguides. *Applied Physics Lett*ers, 73,2,(July,1998) 133-135, 0003-6951

Liang, G. J.; Gong-Wang, S., Huan, M. & Li-Li, H., Qu, L. (2005). Gain and Noise Figure of a Double-Pass Waveguide Amplifier Based on Er/Yb-Doped Phosphate Glass. *Chinese Physics Letter*, 22,11, (July, 2005) 2862-2864, 0256-307x

Lin, H.; Jiang, S., Wu, j., Song, F., Peyghambarian, N. & Pun, E.Y.B. (2003). Er^{3+} doped Na_2O–Nb_2O_5–TeO_2 glasses for optical waveguide laser and amplifier. *Journal of Physics D: Applied Physics*, 36,7, (July, 2003) 812–817,0022-3727

Liu, K. & Pun, E. Y. B. (2009). Comparative studies of spectroscopic properties in Er^{3+}–Yb^{3+} codoped phosphate glasses. *Journal of Alloys and Compounds*, 470, (February, 2009) 340–346, 0925-8388

Liu, K. & Pun, E. Y. B. (2007). Modeling and experiments of packaged Er^{3+}–Yb^{3+} co-doped glass waveguide amplifiers. *Optics Communications*, 273, (May, 2007) 413–420, 0030-4018

Liu, K. & Pun, E. Y. B., (2004). K^+-Na^+ ion-exchanged waveguides in Er^{3+}-Yb^{3+} codoped phosphate glasses using field-assisted annealing. *Applied Optics*, 43, 15, (May, 2004) 3179-3184, 0003-6935

Mariappan, C.R.; Govindaraj, G., Rathan, V. S., & Vijaya Prakash, G. (2005).
(a)Vitrification of $K_3M_2P_3O_{12}$ (M = B, Al, Bi) NASICON-type materials and electrical relaxation studies. Materials Science and Engineering B, 123, (November, 2005) 63-68, 0921-5107
(b)Preparation, characterization, ac conductivity and permittivity studies on vitreous $M_4AlCdP_3O_{12}$ (M = Li, Na, K) system. Materials Science and Engineering B, 121, (July, 2005) 2-8, 0921-5107

Milova, G.; Najafi, S.I., Skirtach, A.G., Simkin, D.J., Andrews, M.P. (1997). *Proceedings of SPIE*, pp.90-101, San Jose, February, 1977, SPIE, USA

Miniscalco, W.J. (1999). Erbium-Doped Glasses for Fiber Amplifiers at 1500 nm. *Journal of Lightwave Technology*, 9, 2, (February, 1991) 234-250, 0733-8724

Mc Cumber, D. E. (1964). Theory of phonon-Terminated optical masers. *Physical Review*, 134, 2A, (November, 1964) A299-A306, 0031-899x

Nandi, P.; Jose, G., Jayakrishnan, C., Debbarma, S., Chalapathi, K., Alti, K., Dharmadhikari, A. K., Dharmadhikari, J. A. & Mathur, D. (2006). Femtosecond laser written channel waveguides in tellurite glass. *Optics Express* 14, 25, (December, 2006) 12145-12150

Najafi, S.I.; Andrews, M.P., Fardad, M.A., Milova, G., Tahar, T., Coudray, P. (1996). *Proceedings of SPIE*, pp.100-104, Berlin, October, 1996, SPIE, Germany

Nakazawa, M. & Kimura, Y. (1992). Electron-beam vapour-deposited erbium-doped glass waveguide laser at 1.53μm. *Electronics Letters*, 28, 22, (October 1992) 2054-2055, 0013-5194

Ning, N.; lv-yun, Y., Ming-ying, P., Qing-ling, Z., Dan-ping, C., Akai, T. & Kadono, K. (2006). Preparation and spectroscopic properties of Er^{3+}-doped high silica glass fabricated by sintering nanoporous glass. *Materials Letters*, 60, (July, 2006) 1987–1989, 0167-577x

Ofelt, G. S. (1962). Intensities of Crystal Spectra of Rare earth Ions. *Journal of Chemical Physics*, 37, 3, (August, 1962) 511-520, 0021-9606

Osellame, R.; Della Valle, G., Chiodo, N., Taccheo, S., Laporta, P., Svelto, O. & Cerullo, G. (2008). Lasing in femtosecond laser written optical waveguides. *Applied physics* A, 93, 1, (October, 2008) 17-26, 0947-8396

Osellame, R. ; Taccheo, S., Marangoni, M., Ramponi, R., Laporta, P., Polli, D., De Silvestri S. & G. Cerullo (2003). Femtosecond writing of active optical waveguides with astigmatically shaped beams. *Journal of the Optical Society of America B: Optical Physics*, 20, 7, (July, 2003) 1559-1567, 0740-3224

Psaila, N. D.; Thomson, R. R., Bookey, H. T., Kar, A. K., Chiodo, N., Osellame, R., Cerullo, G., Jha, A. & Shen, S. (2007). Er:Yb-doped oxyfluoride silicate glass waveguide amplifier fabricated using femtosecond laser inscription. *Applied Physics Letters*, 90, (January, 2007) 131102, 0003-6951

Peters, P. M.; Funk, D. S., Peskin,A.P., Veasey, D.L., Sanford, N.A., Houde-Walter, S.N. & Hayden, J.S. (1999). Ion-exchanged waveguide lasers in $Er^{3+}Yb^{3+}$ codoped silicate glass. *Applied Optics*, 38, 33, (November, 1999) 6879-6886, 0003-6935

Pradeesh, K.; Oton, C.J., Agotiya, V.K., Raghavendra, M., Vijaya Prakash, G. (2008). Optical properties of Er^{3+} doped alkali chlorophosphate glasses for optical amplifiers. *Optical materials*, 31, (October-December, 2008) 155-160, 0925-3467

Ramaswamy, R.V. & Srivastava, R.(2000). Ion exchanged glass wavewguides: A review. *Journal of Lightwave Technology*, 6, 6, (October 2000) 984-1002, 0733-8724

Reisfeld, R. & Jorgensen, C.K. (2007). *Lasers and excited states of rare earths*. Springer-verlag, 0387083243, Berlin, New York.

Righini, G. C.; Pelli, S., Brenci, M., Ferrari, M., Duverger, C., montagna, M. & dallIgna, R. (2001). Active optical waveguides based on Er- and Er/Yb- doped silicate glasses. *Journal of Non-Crystalline Solids*, 284, (May, 2001) 223-229, 0022-3093

Righini, G.C.; Pelli, S., Fossi, M., Brenci, M., Lipovskii, A.A., Kolobkova, E.V., Speghini, A., Bettinelli, M. (2001). Characterzation of Er-doped sodium-niobium phosphate glasses. Proceedings of SPIE, pp.210-215, 9780819439604, USA, April 2001, SPIE, San Jose

Rivera, V. A. G.; Chillcce, E. F., Rodriguez, E., Cesar, C. L. & Barbosa, L. C. (2006). Planar waveguides by ion exchange in Er^{3+}-doped tellurite glass. *Journal of Non-Crystalline Solids*, 352, (May, 2006) 363–367, 0022-3093

Sakida, S.; Nanba, T. & Miura, Y. (2007). Optical properties of Er^{3+} doped tungsten tellurite glass waveguides by Ag^{+}-Na^{+} ion-exchange. *Optical materials*, 30, (2007) 586–593.

Sakida, S.; Nanba, T. & Miura, Y. (2006). Refractive-index profiles and propagation losses of Er^{3+}-doped tungsten tellurite glass waveguide by Ag^{+}–Na^{+} ion-exchange. *Materials Letters*, 60, (December, 2006) 3413–3415, 0167-577x

Salavcova, L.; Svecova, B., janakova, S., Kolek, O., Míka, M., Spirkova, J. & Langrova, (2005). Planar optical waveguides in newly developeder:silicate glasses: a comparative study of $K^{+}$and Ag^{+} ion exchange. *Ceramics – Silikaty*, 49, 1, (September, 2005) 53-57, 0862-5468

Seneschal, K.; Smektala, F., Bureau, B., Floch, M. L., Jiang, S., Luo, T., Lucas, J. & Peyghambarian, N. (2005). Properties and structure of high erbium doped phosphate glass for short optical fibers amplifiers. *Materials Research Bulletin*, 40, (2005) 1433–1442, 0025-5408

Shen, S. & Jha, A. (2004). The influence of F^{-} ion doping on the fluorescence ($^4I_{13/2} \rightarrow {}^4I_{15/2}$) line shape broadening in Er^{3+}-doped oxyfluoride silicate glasses. *Optical Materials*, 25, (April, 2004) 321–333, 0925-3467

Shmulovich, J.; Wong, Y.H., Becker, P.C., Bruce, A.J., Adar, R. & Wong, A. (1992) Er^{3+} glass waveguide amplifier at 1.5 μm on silicon. *Electronics Letters*, 28, (June, 1992) 1181-1182, 0013-5194

Stavrou, E.; Tsiantos, C., Tsopouridou, R.D., Kripotou, S., Kontos, A.G., Raptis, C., Capoen, B., Bouazaoui, M., Turrell, S. & Khatir, S. (2010) Raman scattering boson peak and differential scanning calorimetry studies of the glass transition in tellurium–zinc oxide glasses. *Journal of Physics: Condensed Matter*, 22, 19, (May, 2010) 195103, 0953-8984

Surendra Babu, S.; Babu, P., Jayasankar, C.K., Sievers, W., Troster, Th. & Wortmann, G. (2007). Optical absorption of and photoluminescence studies of Eu^{3+} doped

phosphate and fluorophosphates glasses. *Journal of Luminescence*, 126, (September, 2007), 109-120, 0022-2313.

Surendra Babu, S.; Jang, K., Cho, E.J., Lee, H. & Jayasankar, C.K. (2007). Thermal, structural and optical properties of Eu^{3+} -doped Zinc-tellurite glasses. *Journal of Physics D: Applied Physics*, 40,18, (August, 2007),5767-5774, 0022-3727.

Taccheo, S.; Della Valle, G., Osellame, R., Cerullo, G., Chiodo, N., Laporta, P., Svelto, O., Killi, A., Morgner, I., Lederer, M. & Kopf, D. (2004). Er:Yb-doped waveguide laser fabricated by femtosecond laser pulses. *Optics Letters*, 29, 22, (November, 2004) 2626-2628, 0146-9592

Thomson, R. R.; Bookey, H. T. , Psaila, N., Campbell, S., Reid, D. T., Shen, S., Jha, A., & Kar, A. K. (2006). Internal Gain From an Erbium-Doped Oxyfluoride-Silicate Glass Waveguide Fabricated Using Femtosecond Waveguide Inscription. *IEEE Photonics Technology Letters*, 18, 14, (July, 2006) 1515-1517, 1041-1135

Thomson, R. R.; Campbell, S., Blewett, I. J., Kar, A. K. & Reid, D. T. (2005). Active waveguide fabrication in erbium-doped oxyfluoride silicate glass using femtosecond pulses. *Applied Physics Letters*, 87, (April, 2005) 121102,0003-6951

Valle, G. D.; Osellame, R., Chiodo, N., Taccheo, S., Cerullo, G., Laporta, P., Killi, A., Morgner, U., Lederer, M. & Kopf, M. (2005). C-band waveguide amplifier produced by femtosecond laser writing. *Optics Express*, 13, 16, (August, 2005) 5976-5983, 1094-4087

Veasey, D.L.; Funk, D.S., Peters, P.M., Sanford, N.A., Obarski, G.E., Fontaine, N., Young, M., Peskin, A.P., Liu, W., Houde-Walter, S.N. & Hayden, J. S. (2000). Yb/Er-codoped and Yb-doped waveguide lasers in phosphate Glass. *Journal of Non-Crystalline Solids*, 263&264, (March, 2000) 369±381, 0022-3093

Vijaya Prakash, G.; Jagannathan, R. & Rao, D.N. (2002). Physical and optical properties of NASICON-type phosphate glasses. *Materials Letters*, 57, (November, 2002) 134-140

Vijaya Prakash, G.; Nachimuthu, P., Vithal, V. & Jagannathan, R. (2002). Rare earth fluorescence in NASICON type phosphate glass, $Na_3TiZnP_3O_{12}$. *Bulletin of Material Science*, 22, 2, (March, 2002) 121-127, 0250-4707

Vijaya Prakash, G.; Rao, D.N. & Bhatnagar, K. (2001). Linear optical properties of niobium- based tellurite glasses. *Solid State Communications*, 119, (June, 2001) 39-44, 0038-1098

Vijaya Prakash, G. (2000). Absorption spectral studies of rare earth ions (Pr^{3+}, Nd^{3+}, Sm^{3+}, Dy^{3+}, Ho^{3+} and Er^{3+}) doped in NASICON type phosphate glass, $Na_4AlZnP_3O_{12}$. *Materials Letters*. 46, (October 2000) 15-20, 0167-577x

Vijaya Prakash, G. & Jagannathan, R. (1999). Fluorescence properties of Eu^{3+} doped lead bearing fluoro-chloro phosphate glasses. *Spectrochimica Acta Part A 55*, (August, 1999) 1799–1808, 1386-1425

Vishnubhatla, K.C; Rao, S. V., Kumar, R. S. S., Osellame, R., Bhaktha, S.N.B., Turrell, S., Chiappini, A., Chiasera, A., Ferrari, M., Mattarelli, M., Montagna, M., Ramponi, R., Righini, G.C. & Rao, D.N. (2009). Femtosecond laser direct writing of gratings and waveguides in high quantum efficiency erbium-doped Baccarat

glass. *Journal of Physics D: Applied Physics* 42, 20, (March, 2009) 205106, 0022-3727

Wong, S. F.; Pun, E. Y. B. & Chung, P. S. (2002). Er^{3+}–Yb^{3+} Codoped Phosphate Glass waveguide amplifier using Ag^{+}–Li^{+} ion exchange. *IEEE Photonics Technology Letters*, 14, 1, (January, 2002) 80-82, 1041-1135

Wybourne, B. G. (1965). *Spectroscopic Properties of Rare Earths*, John Wiley, New York

Zhao, S.; Wang, X., Fang, D., Xu, S. & Hu, L. (2006). Spectroscopic properties and thermal stability of Er^{3+}-doped tungsten–tellurite glass for waveguide amplifier application. *Journal of Alloys and Compounds* 424, (November, 2006) 243–246, 0925-8388

Zhang, X.Z.; K. Liu, K., Mu, S. K., Tan, C. Z., Zhang, D., Pun, E.Y.B. & Zhang, D.M. (2006). Er^{3+}–Yb^{3+} co-doped glass waveguide amplifiers using ion-exchange and field assisted annealing. *Optics Communications* 268, (December, 2006) 300–304, 0030-4018

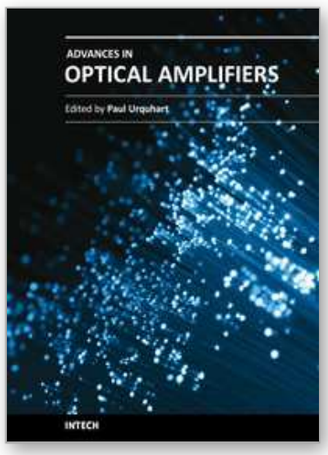

Advances in Optical Amplifiers
Edited by Prof. Paul Urquhart

ISBN 978-953-307-186-2
Hard cover, 436 pages
Publisher InTech
Published online 14, February, 2011
Published in print edition February, 2011

Optical amplifiers play a central role in all categories of fibre communications systems and networks. By compensating for the losses exerted by the transmission medium and the components through which the signals pass, they reduce the need for expensive and slow optical-electrical-optical conversion. The photonic gain media, which are normally based on glass- or semiconductor-based waveguides, can amplify many high speed wavelength division multiplexed channels simultaneously. Recent research has also concentrated on wavelength conversion, switching, demultiplexing in the time domain and other enhanced functions. Advances in Optical Amplifiers presents up to date results on amplifier performance, along with explanations of their relevance, from leading researchers in the field. Its chapters cover amplifiers based on rare earth doped fibres and waveguides, stimulated Raman scattering, nonlinear parametric processes and semiconductor media. Wavelength conversion and other enhanced signal processing functions are also considered in depth. This book is targeted at research, development and design engineers from teams in manufacturing industry, academia and telecommunications service operators.

How to reference
In order to correctly reference this scholarly work, feel free to copy and paste the following:

G. Vijaya Prakash, S. Surendra Babu and A. Amarnath Reddy (2011). Optical Amplifiers from Rare-Earth Co-Doped Glass Waveguides, Advances in Optical Amplifiers, Prof. Paul Urquhart (Ed.), ISBN: 978-953-307-186-2, InTech, Available from: http://www.intechopen.com/books/advances-in-optical-amplifiers/optical-amplifiers-from-rare-earth-co-doped-glass-waveguides

INTECH
open science | open minds

InTech Europe
University Campus STeP Ri
Slavka Krautzeka 83/A
51000 Rijeka, Croatia
Phone: +385 (51) 770 447
Fax: +385 (51) 686 166
www.intechopen.com

InTech China
Unit 405, Office Block, Hotel Equatorial Shanghai
No.65, Yan An Road (West), Shanghai, 200040, China
中国上海市延安西路65号上海国际贵都大饭店办公楼405单元
Phone: +86-21-62489820
Fax: +86-21-62489821

IntechOpen